Turbulence, Heat and Mass Transfer 10

Loss of effectiveness of transverse wall oscillations for drag reduction in pipe flows with Reynolds number

Y. Peet[1], D. Coxe[1] and R. Adrian[1]
[1]*School for Engineering of Matter, Transport and Energy, Arizona State University, 501 E. Tyler Mall, 85255, Tempe, AZ, USA, ypeet@asu.edu*

Abstract – This paper investigates the effect of Reynolds number on drag reduction in a turbulent pipe flow using transverse wall oscillation. Three Reynolds numbers are presented, $Re_\tau = 180, 360$, and 720. The drag reduction values decline from 28.8% at $Re_\tau = 180$ to 22.9% at $Re_\tau = 720$. It is demonstrated that all three Reynolds numbers are effective in suppressing small and intermediate scales of motion in and below the buffer layer; however, large scales of motions are enhanced in the log layer and in the outer layer, an effect that exacerbates with the Reynolds number. A spectral decomposition of a turbulent contribution to bulk mean velocity from Fukagata-Iwamoto-Kasagi identity [1] shows that a comparable amount of drag reduction for all three Reynolds numbers comes from suppressing small and intermediate scales of motion. However, large scales of motion contribute negatively to drag reduction, which causes a loss of performance of transverse wall oscillations with Reynolds number.

1. Introduction

Loss of performance of drag reduction mechanisms with Reynolds number has been previously documented, including using some popular techniques, such as spanwise-wall oscillations and streamwise-traveling waves [2]. However, the reason for this decline of effectiveness remains unclear. Earlier studies were focused on characterizing the mean velocity profile with drag reduction. They attributed the loss of effectiveness to a smaller proportion of the region affected by control to the overall region of the flow as the Reynolds number increases. More recent studies performed a spectral decomposition of the flow with and without drag reduction, and the influence of the so-called large-scale motions [3] on skin friction drag was found important. These studies suggested that the flow control mechanism that targets the near-wall layer is inefficient in suppressing the large scales of motion, which leads to a decreased effectiveness of control as the Reynolds number grows.

Effect of Reynolds number on drag reduction with spanwise wall oscillations was previously investigated for channel flows and boundary layers [2]. Pipe flows, on the other hand, bear an important practical significance for a fuel transportation through pipelines. Moreover, pipe flows represent a fundamental canonical configuration in turbulence research, which was shown to have similarities, but also differences with channel flows and boundary layers [3]. The present paper focuses on characterizing the effect of Reynolds number on a turbulent pipe flow with transverse wall oscillation. The study is performed utilizing a spectral-element Direct Numerical Simulation methodology [4].

2. Problem setup

Flow in a pipe of a length $L = 24R$, where R is a pipe radius, is considered. For each Reynolds number ($Re_\tau = 180, 360$, and 720), we compare two configurations: a standard pipe, with no

wall oscillations, and a pipe where transverse wall oscillations are employed to achieve drag reduction. In controlled cases, the azimuthal pipe wall velocity, $W_{wall}(t)$, varies harmonically in time according to the law,

$$W_{wall}(t) = W_0 \sin(\frac{2\pi}{T_0}t). \quad (1)$$

For all three Reynolds numbers, we set the non-dimensional amplitude and period of wall oscillations in wall units as $W_0^+ = 10$, $T_0^+ = 100$, which provide near-optimum drag reduction values in this range of Reynolds numbers [2].

In the current paper, the incompressible Navier-Stokes equations are numerically solved utilizing the Direct Numerical Simulation (DNS) technique. DNS of uncontrolled and controlled cases for the three Reynolds numbers are performed using an open-source spectral-element method Nek5000. The readers are referred to Ref. [4] for more details on the numerical methodology. Boundary conditions at the pipe wall utilize Dirichlet boundary conditions, with zero wall velocity in the uncontrolled case, and the wall velocity set to $\mathbf{u} = (0, 0, W_{wall}(t))$ in the controlled case, with $W_{wall}(t)$ given by Eq. (1), and the velocity vector $\mathbf{u} = (u_x, u_r, u_\theta)$ containing streamwise, radial, and azimuthal velocity components, respectively. The flow in the present simulations is driven by a constant pressure gradient equal to $dP/dx = -2\,\tau_w/R$, where τ_w is the wall shear stress, fixed in both controlled and uncontrolled configurations of the same Reynolds number. Therefore, the effect of drag reduction is seen through an increased bulk mean velocity U_{bulk} in this setting.

3. Results

3.1 Drag Reduction

Table 1 documents the amount of drag reduction achieved at all three Reynolds numbers, calculated both as the percent increase in bulk velocity, and the percent decrease in skin friction. A decrease of effectivenes of the wall oscillations as the Reynolds number increases is evident.

Table 1: Percent change of bulk mean velocity $\left(\%\Delta U_{bulk} = (U^c_{bulk} - U^u_{bulk})/U^u_{bulk} \cdot 100\%\right)$ and skin friction $\left(\%\Delta C_f = -(C^c_f - C^u_f)/C^u_f \cdot 100\%, C_f = 2\tau_w/(\rho\, U^2_{bulk})\right)$. Superscript "$c$" refers to controlled cases, and "u" to uncontrolled cases.

Re_τ	$\%\Delta U_{bulk}$	ΔC_f
170	18.54	28.8
360	16.25	26.0
720	13.9	22.9

3.2 Turbulence Spectra

Figure 2 presents the difference in the spectra of streamwise kinetic energy, $\overline{u'_x u'_x}/u^2_\tau$, $u_\tau = \sqrt{\tau_w/\rho}$ is the friction velocity, between controlled and uncontrolled cases as a function of wall normal location and the wavelength; λ_x and λ_s denote the streamwise and azimuthal wavelengths, respectively, r is the radial coordinate, and y is the distance from the wall. Superscript "$+$" denotes the normalization in wall units, and superscript "$\star$" denotes the normalization in outer units as, e.g., $\lambda^\star_x = \lambda_x/R$. It can be seen that both small and large streamwise scales of motion are suppressed by the flow control in and below the buffer layer, while the large

streamwise scales of motion with $\lambda_x^+ \gtrsim 5000$ are enhanced in and above the log layer. For the azimuthal scales of motion, the small scales with $\lambda_s^+ \lesssim 500$ are equivalently suppressed in all three Reynolds numbers. However, the larger azimuthal scales, with $\lambda_s^+ \gtrsim 500$ are enhanced all throughout the pipe interior, but especially above the buffer layer. Larger Reynolds number domains allow for a development of a wider range of large-scale structures, whose enhancement, conceivably, contributes negatively to skin friction drag reduction.

Figure 3 documents the difference in the spectra of the Reynolds shear stress, $\overline{u_x' u_r'}/u_\tau^2$, between controlled and uncontrolled cases as a function of wall normal location and the wavelength. One can observe that in and above the buffer layer, Reynolds shear stress contribution in WWO cases is reduced in all the streamwise wavelengths (except for a small set of short streamwise wavelengths $\lambda_x^+ < 500$) to a height of $y^+ \approx 50$, or approximately twice the Stokes' layer width (figures 3a, 3c,3e). Above this region, the streamwise wavelengths of less than $\lambda_x^+ < 5000$ remain attenuated. However, larger scales of motion exhibit significant energy increases in and above the log layer. A similar pattern is observed for the azimuthal spectra of the Reynolds shear stress in Figures 3b, 3d, 3f. Attenuation in the azimuthal wavelengths associated with the azimuthal streak spacing ($\lambda_s^+ \approx 100$) in the buffer layer in the WWO as compared to the NWO cases is pronounced. Enhancement of the large azimuthal scales in the outer layer by wall oscillations can be noted as well. Effect of the Reynolds number seems to be in strengthening of this large-scale enhancement in the outer layer, both for streamwise and azimuthal wavelengths. Additionally, as Reynolds number increases, a fractal-like pattern emerges (blue and red "fingers" visible in the azimuthal spectra), where progressively larger azimuthal scales are being affected (suppressed or enhanced) as the near-wall distance increases, testifying of the influence of wall oscillations on the hierarchy of turbulent structures that form the near-wall attached eddies [5], hairpin packets [6], and very-large-scale motions [7].

3.3 Contribution to Bulk Mean Velocity

Utilizing Fukagata-Iwamoto-Kasagi identity [1], it is possible to decompose the bulk mean velocity as

$$U_{bulk}^+ = \frac{Re_\tau}{4} - Re_\tau \int_0^1 \overline{u_x'^+ u_r'^+} r^{\star 2} dr^\star, \tag{2}$$

$r^\star = r/R$, where the first term represents a laminar contribution (identical between controlled and uncontrolled cases at a fixed Re_τ), and the second term represents the turbulent contribution, U_{bulk}^{t+}. Figure 1 shows the spectra of the difference of the turbulent contribution, ΔU_{bulk}^{t+}, between controlled and uncontrolled cases. Figure 1 shows a significant amount of drag reduction (increase in a non-dimensional bulk mean velocity) in small- to intermediate- streamwise and azimuthal scales of $\lambda_x^+ \lesssim 5000$ and $\lambda_s^+ \lesssim 500$, practically invariant with the Reynolds number, which signifies that this method of flow control is effective in suppressing the near-wall cycle, which it was designed to do. However, the larger scales of motion, $\lambda_x^+ \gtrsim 5000$ and $\lambda_s^+ \gtrsim 500$, contribute negatively to drag reduction, which degrades its efficiency with Reynolds number.

4. Conclusions

The current study documents the results of direct numerical simulation of a turbulent pipe flow with and without transverse wall oscillation for three Reynolds numbers, $Re_\tau = 170, 360$ and 720. It is found that wall oscillation results in an increase of a flow rate by almost 20% and,

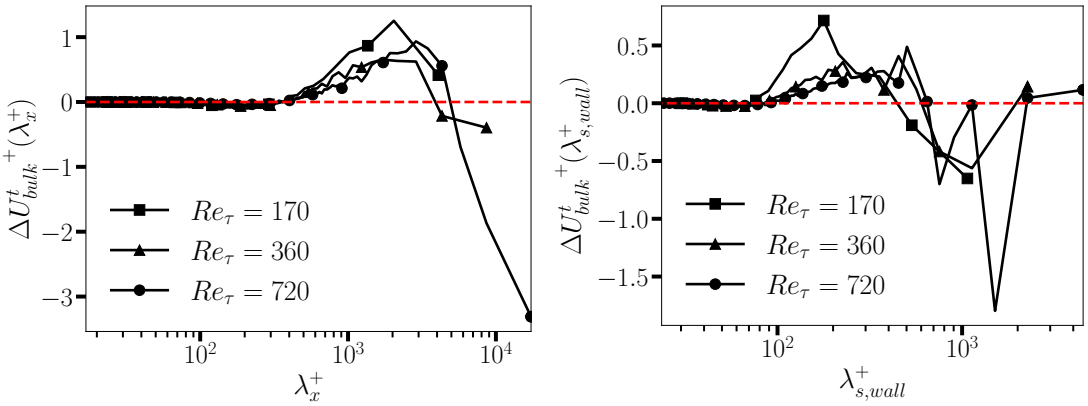

(a) Streamwise spectra

(b) Azimuthal spectra

Figure 1: Spectra of the difference of the turbulent contribution to bulk mean velocity.

consequently, achieves a drag reduction of approximately 30% at the lowest Reynolds number; however, this effect decreases as the Reynolds number increases. Spectra of streamwise kinetic energy, Reynolds shear stress and the turbulent contribution to the bulk mean velocity are analyzed to explain this effect.

It is found that the primary effect of wall oscillation is to reduce the turbulent kinetic energy and Reynolds shear stresses in the intermediate- to large- streamwise and azimuthal scales of motion in the buffer layer of the flow. To the contrary, energy and shear stresses are increased in the large-scale structures in the log layer and the wake region. At the lowest Reynolds number, $Re_\tau = 170$, the inner layer extends through $\approx 65\%$ of the domain while it comprises $\approx 15\%$ of the domain at $Re_\tau = 720$. Since the overall attenuation of energetic structures is limited to the inner layer of the flow, this explains the reduced effectiveness of the wall oscillation as a drag reduction mechanism as the Reynolds number increases.

The analysis of the contribution to the bulk mean velocity based on the Fukagata-Iwamoto-Kasagi identity [1] shows a good collapse of the difference in its spectra between the uncontrolled and controlled cases across all three Reynolds numbers, showing that the drag reduction is limited to the streamwise wavelengths of $\lambda_x^+ < 5000$ independent of the Reynolds number. The wavelengths with $\lambda_x^+ > 5000$, which are progressively more dominant at high Reynolds numbers, lead to a drag increase. This observation can lead to a conclusion that drag reduction mechanisms that are optimized at reducing near-wall turbulence at low Reynolds number may not necessarily be as effective at higher Reynolds numbers since they fail to control the large scales of motions. Perhaps, different drag reduction strategies, targeted at larger-scale structures [10, 11], can yield a better performance at high Reynolds numbers.

Acknowledgements

This research was supported by the NSF CAREER award # CBET-1944568 and by the Ira A. Fulton Professorship endowment.

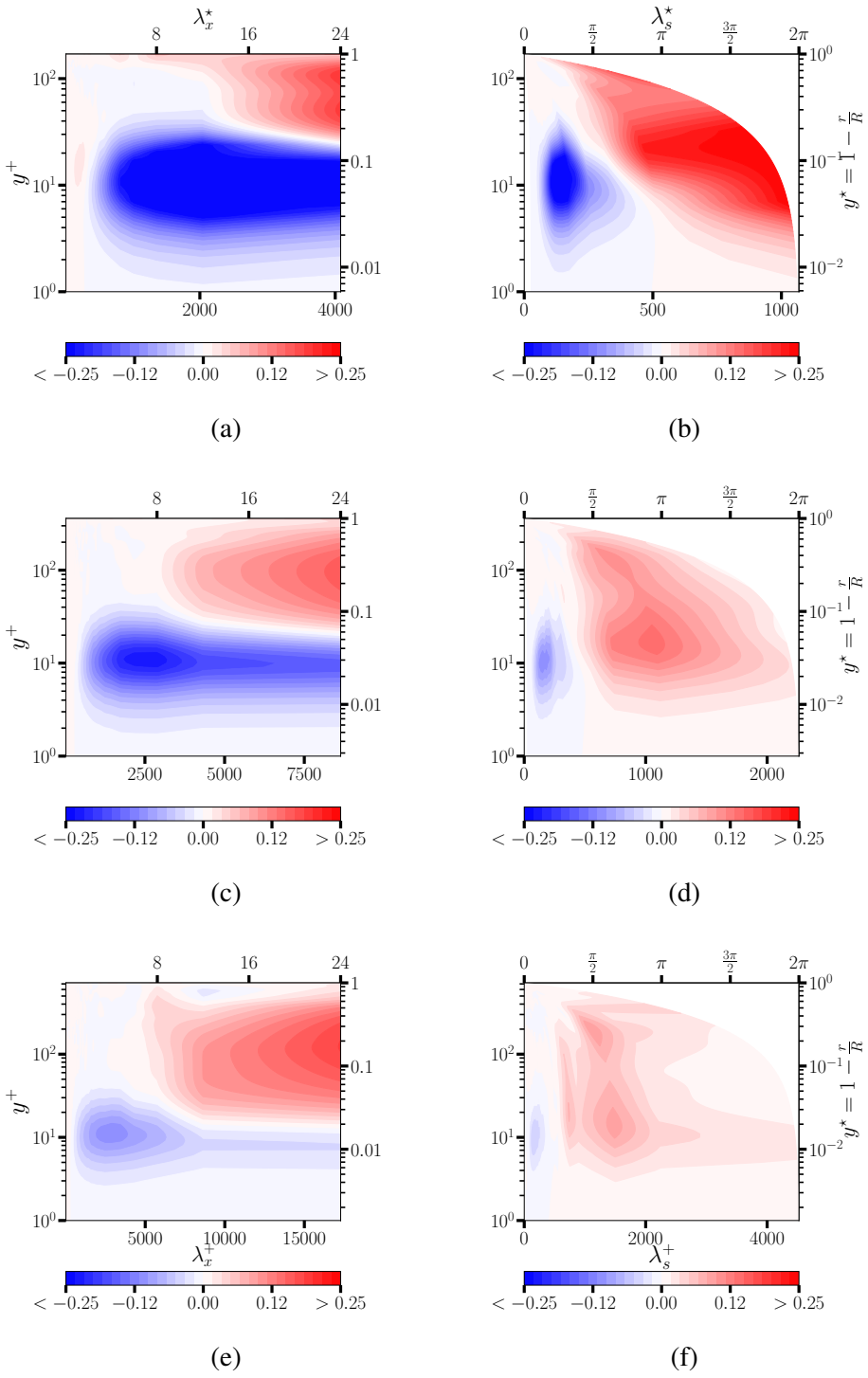

Figure 2: Difference in the spectra of streamwise kinetic energy between controlled and uncontrolled cases as a function of wall normal location and the wavelength: (a,c,e) streamwise spectra; (b,d,f) azimuthal spectra. From top to bottom: (a,b) $Re_\tau = 170$, (c,d) $Re_\tau = 360$, and (e,f) $Re_\tau = 720$.

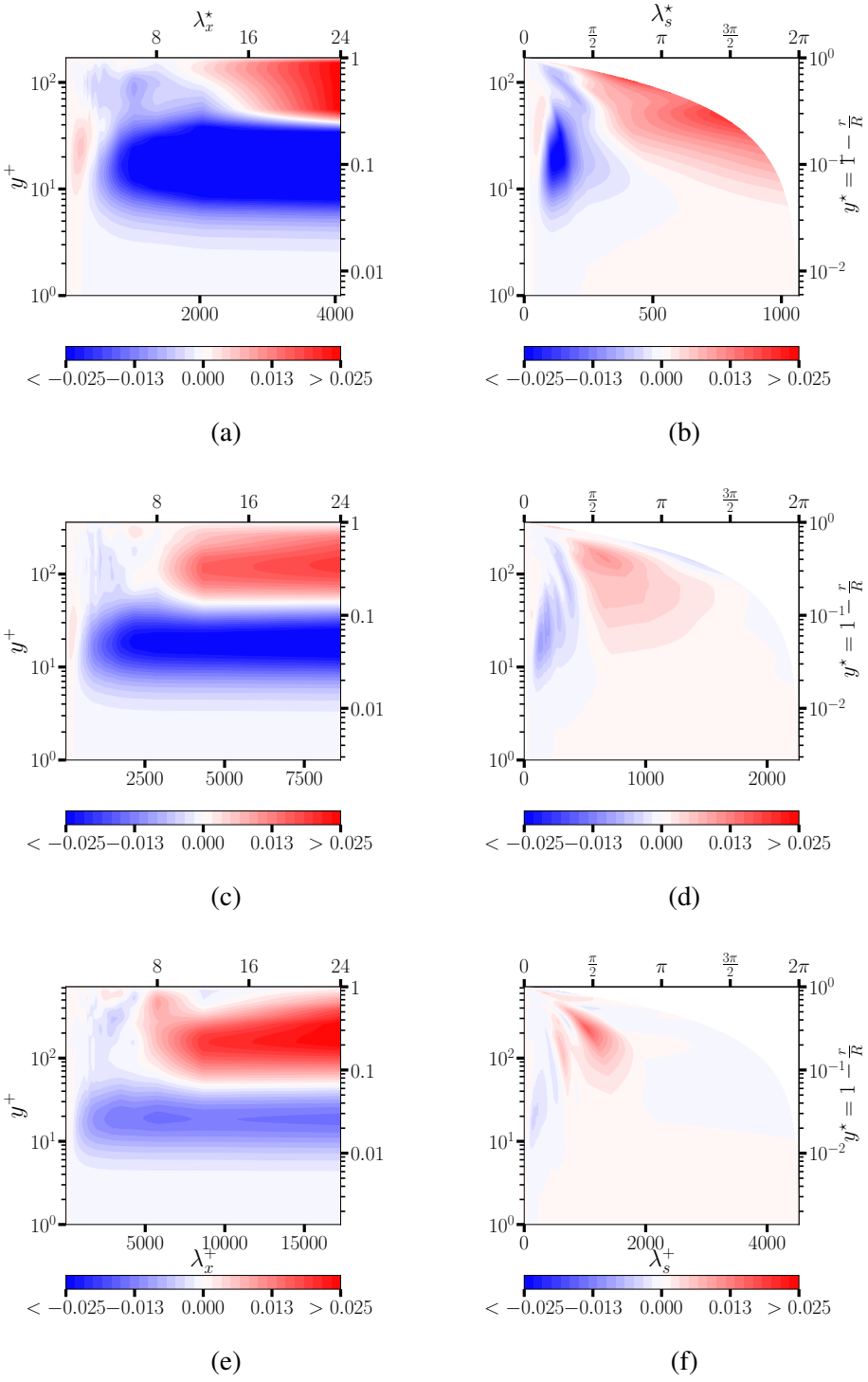

Figure 3: Difference in the spectra of Reynolds shear stress between controlled and uncontrolled cases as a function of wall normal location and the wavelength: (a,c,e) streamwise spectra; (b,d,f) azimuthal spectra. From top to bottom: (a,b) $Re_\tau = 170$, (c,d) $Re_\tau = 360$, and (e,f) $Re_\tau = 720$.

References

1. K. Fukagata, K. Iwamoto and N. Kasagi. Contribution of Reynolds stress distribution to the skin friction in wall-bounded flows. *Phys. Fluids*, 14(11):L73–L76, 2002.
2. P. Ricco, M. Scote and M. Leschziner. A review of turbulent skin-friction drag reduction by near-wall transverse forcing. *Progr. Aero. Sci.*, 123:100713, 2021.
3. A. Smits, B. McKeon and I. Marusic. High–Reynolds number wall turbulence. *Ann. Rev. Fluid Mech.*, 43:353–375, 2011.
4. M. Deville, P. Fischer and H. Mund. High-Order Methods for Incompressible Fluid Flow. Cambridge University Press, 2002.
5. A. A. Townsend. The structure of the turbulent boundary layer. *Mathematical Proceedings of the Cambridge Philosophical Society*, 47:375–395, 1951.
6. R. J. Adrian. Hairpin vortex organization in wall turbulence. *Physics of Fluids*, 19:041301, 2007.
7. B. J. Balakumar and R. J. Adrian. Large-and very-large-scale motions in channel and boundary-layer flows. *Philosophical Transactions of the Royal Society A: Mathematical, Physical and Engineering Sciences*, 365:665–681, 2007.
8. Y. Hwang. Statistical structure of self-sustaining attached eddies in turbulent channel flow. *Journal of Fluid Mechanics*, 767:254–289, 2015.
9. M. Guala, S. E. Hommema and R. J. Adrian. Statistical structure of self-sustaining attached eddies in turbulent channel flow. *Journal of Fluid Mechanics*, 554:521–542, 2006.
10. M. R. Abbassi, W. J. Baars, N. Hutchins and I. Marusic. Skin-friction drag reduction in a high-Reynolds-number turbulent boundary layer via real-time control of large-scale structures. *International Journal of Heat and Fluid Flow*, 67:30–41, 2017.
11. I. Marusic, D. Chandran, A. Rouhi, M. K. Fu, D. Win, B. Holloway, D. Chung and A. J. Smits. An energy-efficient pathway to turbulent drag reduction. *Nature Communications*, 12:1–8, 2021.